COMPARISON OF MGS RADIO SCIENCE MEAN TEMPERATURE PROFILES WITH MARS CLIMATE SOUNDER (MCS) RESULTS

J. H. Shirley, J. T. Schofield, A. Kleinböhl, D. Kass, D. J. McCleese, J. Benson, and P. Wolkenberg, *California Institute of Technology-Jet Propulsion Laboratory, Pasadena CA USA (James.H.Shirley@jpl.nasa.gov).*

Introduction: Observations of the Mars atmosphere have been obtained by a variety of remote sensing techniques and instruments during the past three decades. In order to obtain a consistent picture of the variability of the Mars atmosphere with time it is necessary to "cross-validate" the observations from different instruments and investigations.

Atmospheric temperature retrievals obtained by the Radio Science Experiment on the Mars Global Surveyor (MGS) spacecraft are widely considered to represent the best available solutions for Mars years 24-27. However, the spatial and temporal coverage of the MGS RS dataset is limited to those locations and times of spacecraft occultations. Hinson, Smith and Conrath (2004) presented detailed comparisons of the MGS RS profiles with contemporaneous profiles obtained by the MGS Thermal Emission Spectrometer (TES), finding good agreement (within ~ 2 K) at pressures < 400 Pa. Among other results, they noted that TES profiles were consistently warmer than the RS solutions in the lowest scale height (~10 km) of the atmosphere.

The Mars Reconnaissance Orbiter (MRO) Mars Climate Sounder (MCS) instrument (McCleese et al. 2007) began observing in September 2006 (L_s 111 of MY 28). While there are no contemporaneous MGS-RS occultations and MCS observations, it is nonetheless important to compare the solutions for atmospheric temperatures obtained by these two investigations at similar seasons and in similar locations. Such comparisons aid in understanding the strengths and limitations of both datasets. Because the MCS atmospheric retrievals algorithms (Kleinböhl et al. 2009) are continuously under development, such comparisons may also help refine the retrieval algorithms. In addition, comparisons between MGS-RS and MRO-MCS can shed light on the interannual variability of the Mars atmosphere, which is still poorly understood.

Approach: We compare averaged MRO-MCS temperature profiles with averaged MGS-RS temperature profiles for four different L_s intervals where a reasonable number of RS profiles are available. We have interpolated the MGS-RS profiles to the MCS pressure grid for these comparisons. We look first at profiles and zonal averages for northern middle latitudes in the late northern spring season (L_s 70-80). Atmospheric conditions are reasonably settled and aerosol opacities are relatively low in this interval, permitting the comparison of temperature profiles obtained in near-optimum conditions for MCS observations. We next compare MCS results with RS samples from high northern latitudes (75-80 N) during midwinter (L_s 295-300). The corresponding case of high southern latitudes (72-77 S) in midwinter (L_s 105-115) is then examined. These cases allow us to compare MGS-RS and MCS profiles under conditions where temperatures are comparable to the CO_2 condensation temperature. Finally, we also compare two sets of profiles from equatorial latitudes at one specific season (L_s 145-150). Profiles from the Tharsis region are compared with profiles from a lowlands sector (Chryse Planitia). Hinson & Wilson (2004) noted the presence of inversions at pressure levels of 30-200 Pa above elevated terrain during this season. The peak magnitude of the inversion was noted over the Tharsis region. The MCS data for Tharsis and for equatorial lowland locations in this season support these earlier results.

Northern spring comparison: Figure 1 reveals very good agreement of MGS-RS and MCS temperature profiles for this season and latitude.

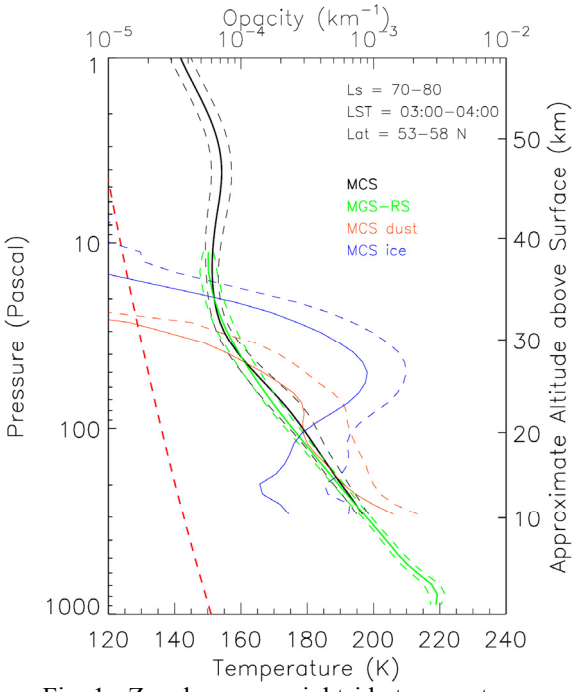

Fig. 1. Zonal average nightside temperature profiles for MGS-RS (green, average of 226 profiles, MY 26) and MRO-MCS (black, average of 1008 profiles, MY 29) in the late northern spring season. The dashed lines are 1-σ error bounds. The dashed red line represents the CO_2 condensation temperature. Profiles of MCS dust and ice opacity are also provided (brown and blue curves with 1-σ upper

bounds; note opacity scale at top).

The MCS retrieval algorithms also provide information on dust and water ice opacities for each profile. The retrieved water ice opacity of Fig. 1 peaks near an altitude of ~25 km, while retrieved dust opacity peaks (and dominates) at much lower levels (~10 km). This general pattern is observed frequently at this season and latitude. The MCS mean profile of Fig. 1 does not extend as deep into the atmosphere as the RS profile, because MCS was operating in "limb staring" mode. The instrument was not obtaining off-nadir views during this interval due to elevation actuator anomaly investigations.

Winter high latitudes comparsions (Northern hemisphere): Figure 2 compares MGS-RS profiles with MCS temperature profiles at latitudes north of the terminator (i.e., in "polar night"). For this comparison the temperatures at the tops of the individual RS profiles have been adjusted to match the average MCS temperature at the same level. (RS temperatures at the uppermost pressure level in standard catalogs derive from estimates based on climatology or other information).

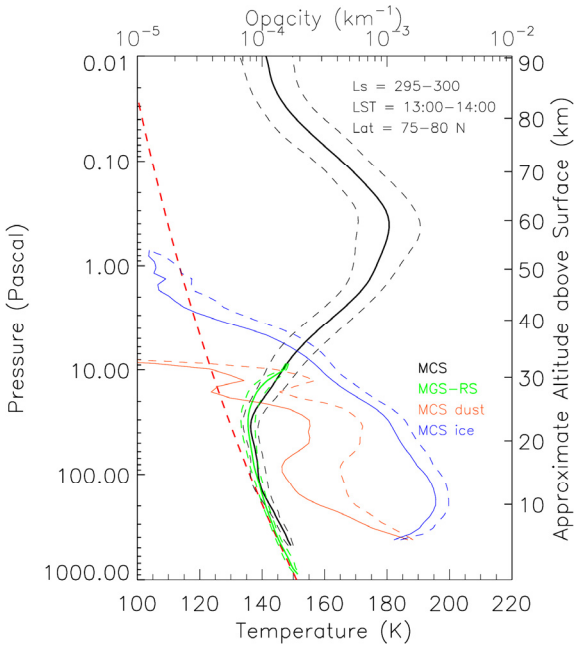

Fig. 2. Zonal average polar night temperature profiles for MGS-RS (green, 88 profiles, MY 27) and MRO-MCS (black, 107 profiles, MY 29) in northern winter. The dashed lines are 1-σ error bounds (only upper bounds are provided for the water ice and dust profiles). The dashed red line represents the CO_2 condensation temperature. The dust opacity profile most probably represents a mixture of CO_2 ice and dust in this case (see discussion in text).

The temperature differences between MGS-RS and MCS are slightly larger between 20 and 30 km altitude than was the case for Fig. 1. This may represent interannual variability. Differences in the vertical resolution of MCS (5 km) and MGS RS (~1 km) may also play a role, as the curvature of the retrieved MCS profile is constrained by temperature values from significantly higher and lower levels. Both profiles closely track the CO_2 condensation temperature below about 15 km altitude.

The MCS retrievals algorithms do not yet retrieve CO_2 cloud opacities (this capability is under development). When temperatures are within 10 K of the CO_2 condensation temperature, the current MCS water ice and dust opacity profiles may be untrustworthy. The opacity profile labeled "MCS dust" in Fig. 2 probably includes contributions from CO_2 and from dust within the Mars winter polar atmosphere. The dust+CO_2 opacity shown in Fig. 2 drops rapidly above 25 km, where the temperatures have risen well above the CO_2 condensation temperature.

Winter high latitudes comparsions (Southern hemisphere): The temperature profiles of Fig. 3 for the southern hemisphere polar night case are similar to those of Fig. 2 for the northern hemisphere. However, in this case the temperature difference between the MGS-RS profile and the MCS profile is considerably larger (~10 K) at ~20 km. Because the latitudes sampled are near the polar vortex, it is possible that differences in the circulation of the atmosphere in the two Mars years sampled (MY 24 and MY 29) may largely account for the difference in temperatures and in the shapes of the mean temperature profiles.

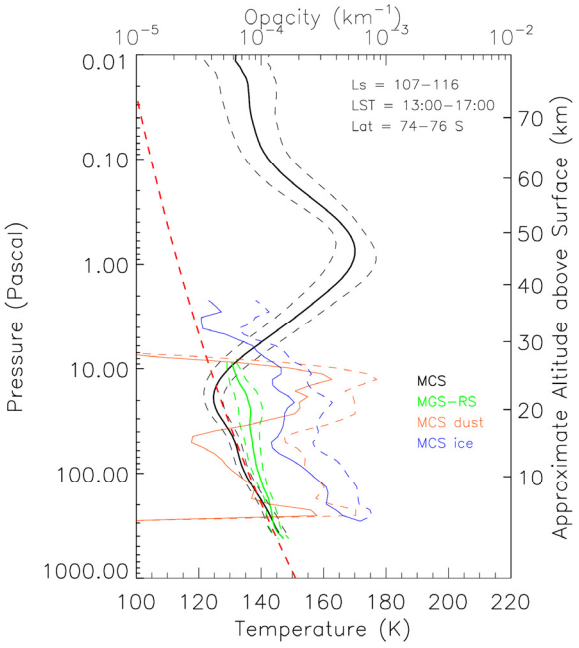

Fig. 3. Zonal average polar night temperature profiles for MGS-RS (green, 49 profiles, MY 24) and MRO-MCS (black, 227 profiles, MY 29) in southern winter. The dashed lines are 1-σ error bounds (only upper bounds are provided for the water ice and dust profiles). The dashed red line represents the CO_2 condensation temperature. The

dust opacity profile more likely represents CO_2 ice and dust opacity in this particular case.

In addition, there is a significant enhancement of Ar and N_2 in the southern polar night winter atmosphere that has not been taken into account for the RS solutions in this case. Taking these species into account may reduce the RS temperatures by several degrees (D. Hinson, personal communication).

As with Fig. 2, the opacity associated with dust and CO_2 ice in Fig. 3 drops rapidly as the temperatures rise significantly above the CO_2 condensation temperature at about 27 km altitude. The MCS mean temperature profile attains temperatures a few degrees colder than the CO_2 condensation temperature between 10 and 20 km altitude. This overshoot may in part arise as a consequence of the 5-km vertical resolution of MCS, as it occurs at an altitude of significant curvature of the profile.

Equatorial lowlands temperature profiles: Figure 4 provides mean MGS-RS and MCS temperature profiles for a 30º longitudinal sector of Mars' equatorial lowlands. As in Figs. 2-3 the top level temperature for the RS profiles was adjusted to the mean for the MCS profiles at that altitude. The higher vertical resolution of the MGS-RS data yields more complex structure than is routinely resolved by MCS. The frequent presence of water ice clouds with significant opacities in equatorial latitudes reduces the total number of MCS profiles available for averaging. Thus observational effects may also play a role in accounting for the temperature differences. Nonetheless the available MCS temperatures are once again in good agreement with those obtained from radio occultations.

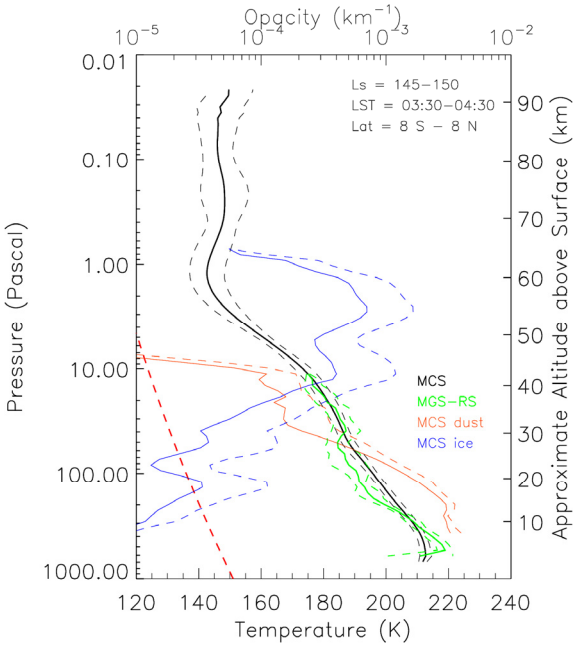

Fig. 4. Mean temperature profiles for MGS-RS (green, 7 profiles, MY 24) and MRO-MCS (black, 35 profiles, MY 29) for equatorial lowlands (Elysium Planitia, longitude 165-180 E, latitudes 8 S – 8 N) from L_s 145-150. The dashed lines are 1-σ error bounds (only upper bounds are provided for the water ice and dust profiles). The dashed red line represents the CO_2 condensation temperature.

The profiles of water ice and dust opacity shown in Fig. 4 are similar to those of Fig. 1, where the dust component dominates at lower altitudes while the water ice makes a greater contribution higher up.

Equatorial highlands temperature comparison: Hinson & Wilson (2004) highlighted an important difference between equatorial temperature profiles obtained by the MGS radio science experiment. Nighttime profiles obtained above elevated terrain from L_s 145-150 tended to exhibit strong temperature inversions, while fewer and weaker inversions were present over equatorial lowlands. The profiles of Figs. 4 and 5 allow us to explore the suggested relationship using data that was not available to Hinson & Wilson (2004).

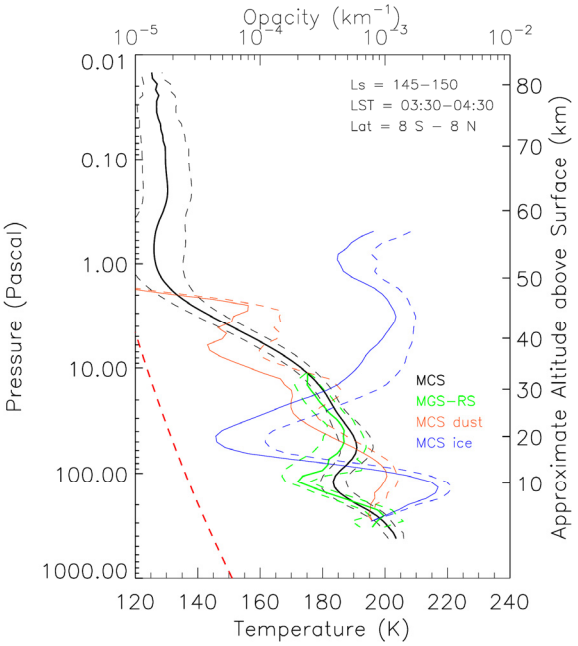

Fig. 5. Mean temperature profiles for MGS-RS (green, 9 profiles, MY 24) and MRO-MCS (black, 28 profiles, MY 29) for equatorial highlands (Tharsis, longitude 240-270 E, latitudes 8 S – 8 N) from L_s 145-150. The dashed lines are 1-σ error bounds (only upper bounds are provided for the water ice and dust profiles). The dashed red line represents the CO_2 condensation temperature. The uppermost temperature values for the individual MGS-RS profiles were adjusted to match the mean MCS temperature at that altitude.

Fig. 5 shows the strong temperature inversion at ~10 km altitude that was noted previously (green curve, MGS-RS). The MCS dataset (black) shows a similar inversion of lesser magnitude at the same altitude in the atmosphere. Once again we suspect that the lower vertical resolution of MCS (5 km ver-

sus ~1 km) has resulted in smoothing out the vertical structure to some degree. The inversion present in Fig. 5 contrasts strongly with the approximately monotonic mean profiles shown in Fig. 4, which are derived from profiles obtained at the same season but over equatorial lowlands rather than over Tharsis.

The water ice opacity profile of Fig. 5 shows remarkable structure, with peak opacity nearly coincident in altitude with the temperature inversion. As in Fig. 4, we must be aware of possible selection effects. It is likely that the mean opacity of water ice at 10 km altitude over Tharsis is even higher than is shown here, due to the fact that many MCS profiles with significant opacity have been excluded from consideration by the MCS quality control procedures.

Discussion: Preliminary comparisons of MRO Mars Climate Sounder mean temperature profiles with MGS Radio Science mean temperature profiles reveal satisfactory agreement between them for various seasons and locations on Mars. Because the MGS and MRO observations are not contemporaneous, it is difficult to separate the effects of interannual variability from possible retrieval biases or other systematic effects that may be present. Ongoing comparisons with MRO radio science occultation profiles will address this question. Additional quantitative information on the profiles presented here will be provided at the workshop and in subsequent publications. Additional comparisons for other locations and seasons are under way.

Acknowledgements: We thank D. Hinson and J. Wilson for critical comments on earlier versions of this presentation. This work was performed at the California Institute of Technology-Jet Propulsion Laboratory under a contract with NASA.

References:

Hinson, D. P., M. D. Smith, and J. J. Conrath 2004, Comparison of atmospheric temperatures obtained through infrared sounding and radio occultation by Mars Global Surveyor, J. Geophys. Res. 109, E1002, doi:10.1029/2004JE002344.

Hinson, D.P., and R. J. Wilson 2004. Temperature inversions,thermal tides, and water ice clouds in the Martian tropics, J. Geophys. Res.109, E01002, doi:10.1029/2003JE002129.

Kleinböhl, A., J. T. Schofield, D. M. Kass, W. A. Abdou, C. R. Backus, B. Sen, J. H. Shirley,W. G. Lawson, M. I. Richardson, F. W. Taylor, N. A. Teanby, and D. J. McCleese 2009. Mars Climate Sounder limb profile retrieval of atmospheric temperature, pressure, dust and water ice opacity. *J. Geophys. Res.*, 114, E10006, doi:10.1029/2009JE003358.

McCleese, D. J., Schofield, J.T., Taylor, F.W., Calcutt, S.B., Foote M.C., Kass, D.M., Leovy, C.B., Paige, D.A., Read, P.L., and Zurek, R.W. 2007. "Mars Climate Sounder: An Investigation of Thermal and Water Vapor Structure, Dust and Condensate Distributions in the Atmosphere, and Energy Balance of the Polar Regions," *J. Geophys. Res.,* Vol. 112, E05S06, doi:10.1029/2006JE002790.